

entire HIV-1 RNA genome, which contains a dazzling 9,173 nucleotides.

The structured regions of the HIV-1 genome are concentrated in about 21 large domains¹. Most of the functionally important structured RNA motifs that have been characterized so far reside in the untranslated (non-protein coding) region near the ends of the viral genome, which regulates viral replication and packaging of viral particles. Watts and colleagues¹ detect these previously characterized RNA motifs, sometimes as components of larger motifs, but they also identify structured RNA elements in protein-coding regions of the genome.

Many HIV-1 proteins are translated into polyprotein precursors by the ribosome as the viral RNA passes through it. The proteins are joined like beads on a string by linker peptides: these are later cleaved to release the individual proteins. There are also unstructured linker peptides between domains that make up the individual HIV proteins. Intriguingly, many of the newly identified structured RNA elements are located in regions that code for these flexible linkers. The authors propose that the structured RNAs slow down protein translation because these regions must be unfolded prior to entry into the ribosome. Because HIV proteins might be folded during translation — a process referred to as co-translational protein folding — this ribosomal pausing may provide additional time for proteins to adopt their correct three-dimensional structures.

This fascinating relationship between RNA and protein structure is not without precedent. The correlation between the secondary structure of messenger RNA and protein translation was recognized as early as three decades ago, and there are several studies showing that mRNA secondary structure can promote ribosomal pausing and modulate other aspects of translation and protein folding⁵. Watts and colleagues¹ go on to identify several other pause sites that seem to buy time at strategic moments during translation. For instance, unwinding folded RNA may allow binding of the signal-recognition particle to the elongating peptide chain. This protein-RNA particle guides the ribosome-peptide-chain complex to the endoplasmic reticulum for further processing. Ribosomal pausing may also provide time for frameshifting — whereby the ribosome stalls and skips over nucleotides without translating them, changing the reading frame — which allows translation of alternative HIV proteins from the same RNA.

On the other hand, highly unstructured regions are observed in hypervariable regions of the HIV-1 genome, which have important roles in viral host evasion. These unstructured regions are bordered by conserved and stable RNA structures that may help to prevent their interaction with the less variable neighbouring regions.

Whenever possible, Watts *et al.*¹ interpreted the details of the SHAPE model in relation to other biochemical and structural data, and

information about evolutionary conservation of the pairing possibility of nucleotide regions. But there are still potential sources of error, particularly for an RNA structure of this size. Many regions probably do not exist as a single secondary structure, instead alternating between different conformations. The SHAPE-directed folding algorithm also fails to recognize some RNA structures, such as pseudoknots, or base pairs that form only as part of higher-order tertiary interactions. Atypical RNA structures may also interfere with the SHAPE analysis.

Notwithstanding these limitations, the study by Watts *et al.*¹ is a considerable achievement, showing the feasibility of obtaining 'aerial' views of large genomic RNA structures that reveal their architecture and possible functions. Structural biologists can now use this genomic map to judiciously zoom in on pieces

of the HIV-1 genome and determine architectural and functional principles at the atomic level. Bridging these disparate RNA structure-function scales as well as moving towards movies of the genome in functional motion will be challenges for the future. But for now, it seems that the quest for a high-resolution structure of the entire HIV-1 RNA genome has begun in earnest. ■

Hashim M. Al-Hashimi is in the Department of Chemistry and Biophysics, University of Michigan, Ann Arbor, Michigan 48109-1055, USA. e-mail: hashimi@umich.edu

1. Watts, J. M. *et al.* *Nature* **460**, 711–716 (2009).
2. Ehresmann, C. *et al.* *Nucleic Acids Res.* **15**, 9109–9128 (1987).
3. Mathews, D. H. *et al.* *Proc. Natl Acad. Sci. USA* **101**, 7287–7292 (2004).
4. Deigan, K. E., Li, T. W., Mathews, D. H. & Weeks, K. M. *Proc. Natl Acad. Sci. USA* **106**, 97–102 (2009).
5. Kozak, M. *Gene* **361**, 13–37 (2005).

BIOGEOCHEMISTRY

Carbonate rocks deconstructed

Michael A. Arthur

The ratios of stable isotopes, especially isotopes of carbon and oxygen, have tales to tell about Earth's history. Post-depositional alteration of the carbonate rocks being studied may radically alter the story.

In a paper reminiscent of a scene from the movie *Total Recall*, in which Arnold Schwarzenegger rapidly terraforms Mars, Knauth and Kennedy (page 728 of this issue)¹ suggest that the 'greening' of Earth started about 850 million years ago in coastal regions. Their thinking is that the spread of photosynthetic life to the land then altered the chemical breakdown of rocks on Earth's surface², increasing the nutrient flux from land to ocean, and resulting in greater sequestration of organic matter in soils and marine sediments. A consequence of that, a hypothesized increase in atmospheric oxygen³, would have set the stage for a subsequent and prolific increase in animal diversity.

These are intriguing ideas. Not least, Knauth and Kennedy provide a plausible explanation for the popular notion that oxygen levels increased substantially in the Neoproterozoic³, the era that runs roughly from 1,000 million to 570 million years ago. But their conclusions will be controversial for at least two reasons.

First, Knauth and Kennedy present no direct evidence for the existence of a widespread terrestrial flora in the Neoproterozoic. Rather, in a creative step, they indirectly infer the occurrence of land colonization by photosynthetic organisms from changing geochemical patterns, as seen in stable isotopes of carbon, in Neoproterozoic shallow-marine carbonate rocks. Second, the authors argue that such rocks have nearly all experienced significant

post-depositional alteration. In doing so, they cast doubt on the many studies that have aimed to reconstruct environmental conditions from the geochemical signals thought to have been locked in at the time that these carbonates were deposited. Their study even brings into question elements of the popular 'snowball Earth' hypothesis⁴, which depends, in part, on the evidence for extreme variations in stable carbon isotopes from some of these same rocks.

So what exactly have Knauth and Kennedy done? Working from published sources, they have generated crossplots of the values of $\delta^{13}\text{C}$ (a measure of the ratio of ^{13}C to ^{12}C) and $\delta^{18}\text{O}$ (a measure of the ratio of ^{18}O to ^{16}O) in shallow-water limestones. They suggest that there is little difference between the distribution of values for much of the Neoproterozoic and the ensuing Phanerozoic, the interval that runs from 570 million years ago to the present. Thus, they argue, the post-depositional alteration (diagenesis) pathways and conditions for modern, Phanerozoic and most Neoproterozoic shallow-marine carbonates were the same.

Knauth and Kennedy¹ point out that, because of periodic falls in sea level, most recent and Phanerozoic shallow-marine carbonate rocks experienced extensive alteration through the action of fresh water. Fresh water percolates through such limestones, either in the near-surface unsaturated zone, or as ground-water 'lenses' that mix with sea water at their

periphery. These low-salinity fluids drive dissolution of the more-soluble primary carbonates (typically aragonite and high-magnesium calcite today) and reprecipitation of less-soluble, low-magnesium calcite as cements and/or replacement minerals. These secondary calcites are lower in $\delta^{18}\text{O}$ because fresh water is depleted in ^{18}O relative to sea water. They are also lower in $\delta^{13}\text{C}$ because of the addition of soil-derived carbon dioxide, resulting from degradation (oxidation) of plant-derived organic matter that is highly depleted in ^{13}C , to the diagenetic fluids. With increasing addition of secondary cements, the bulk-rock, stable-isotope values decrease along a 'lithification' trend.

The authors¹ hypothesize that the paucity of $\delta^{13}\text{C}$ values lower than 0 parts per thousand (‰) in samples older than 850 million years, and the strong similarity between $\delta^{13}\text{C}$ distributions for carbonate rocks after this time in both the Neoproterozoic and Phanerozoic, indicate that a terrestrial biosphere was established by about 850 million years ago. In other words, the lower $\delta^{13}\text{C}$ values of late Neoproterozoic carbonate rocks, which are similar to those in the Phanerozoic, constitute evidence that there was a widespread photosynthetic biota, in coastal regions at least.

Indeed, it has long been appreciated that many shallow-water carbonate sediments experience changes that produce pronounced decreases in both the carbon and oxygen isotope values of the bulk rock^{5,6}. Likewise, in reconstructing diagenetic history, carbonate sedimentologists have commonly used $\delta^{13}\text{C}$ – $\delta^{18}\text{O}$ crossplots in studies of ancient carbonate rocks^{7,8}, including strata from the Proterozoic (which began 2,500 million years ago)⁹. Many such studies have used more than just stable isotopes to track diagenesis, and hint at complications. For example, the presence of concentrations of trace elements such as strontium, manganese and iron, as well as cathodoluminescence microscopy, have been used to eliminate heavily altered samples from consideration in interpreting primary seawater chemistry. Manganese and iron substitute into secondary carbonates because of the reducing conditions that characterize many subsurface diagenetic fluids. However, their incorporation in primary precipitates may also have occurred during the Proterozoic because of widespread deeper anoxic conditions and low sulphate concentrations³. Thus, the normal signals for carbonate diagenesis may not be entirely

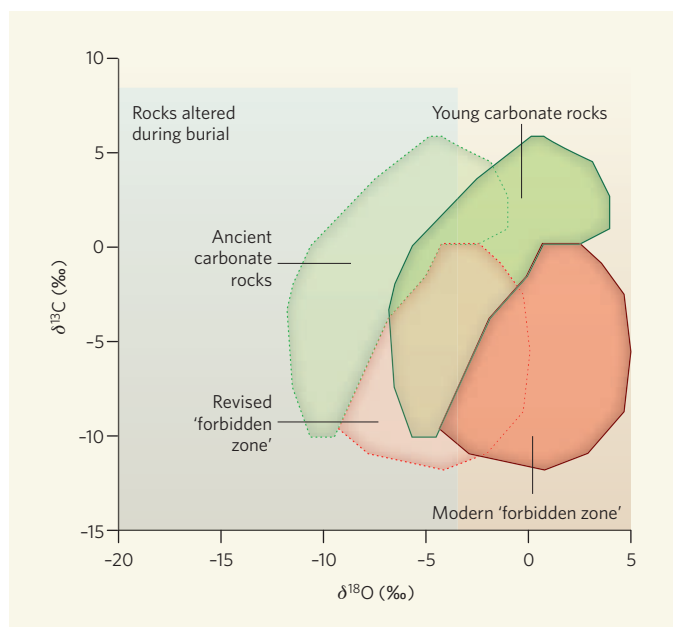


Figure 1 | Crossplot fields of $\delta^{13}\text{C}$ and $\delta^{18}\text{O}$ for shallow-marine carbonate rocks, and the 'forbidden zone'. Dark green, crossplot fields for young — modern — and many Phanerozoic rocks that have undergone alteration by 'freshwater' diagenesis soon after deposition. Light green, postulated field for ancient — some Phanerozoic and most Neoproterozoic — rocks that have experienced 'freshwater' diagenesis but were deposited with initially lower $\delta^{18}\text{O}$ values relative to modern rocks. The blue shaded zone delimits the crossplot area in which the original isotope values in the rock are thought to have become diagenetically altered (overprinted) during burial. Knauth and Kennedy¹ suggest that ancient carbonate rocks with extremely low carbon isotope values, which might indicate lack of overprinting alteration, should fall in a 'forbidden zone' (dark red). Few samples of ancient carbonate rocks fall in this zone, as defined by modern seawater conditions. But a challenge to the authors' assumption arises from the case that, in the past, combinations of lower average oxygen isotope values in sea water, and warmer temperatures, might plausibly have produced a $\delta^{18}\text{O}$ that was shifted 5‰ lower (light red). Many values for ancient carbonate rocks would then fall in this revised forbidden zone. Thus, they could represent relatively unaltered samples indicative of the carbon isotopic values for ancient sea water at the time.

applicable to these older rocks.

Knauth and Kennedy¹, however, make certain assumptions about the primary values of $\delta^{18}\text{O}$ in all Neoproterozoic (and Phanerozoic) carbonates. In particular, they tacitly assume that the temperature and $\delta^{18}\text{O}$ of sea water in tropical to subtropical environments has not varied significantly through time. Thus, they expect that primary precipitates should have 'modern' values of $\delta^{18}\text{O}$ (actually, quite ^{18}O -enriched) (Fig. 1). This allows them to posit that the lack of Neoproterozoic samples that fall in their 'forbidden zone' (high $\delta^{18}\text{O}$ and low $\delta^{13}\text{C}$ values) indicates that the carbonate $\delta^{13}\text{C}$ values as low as -10‰ , which some workers interpret as major perturbations of the $\delta^{13}\text{C}$ of seawater-dissolved inorganic carbon, possibly reflect a high degree of alteration.

Moving the 'modern' marine-lithification trend towards lower $\delta^{18}\text{O}$ values (Fig. 1), however, could change that interpretation. For example, if seawater $\delta^{18}\text{O}$ was somewhat lower or low-latitude temperatures warmer, primary carbonate $\delta^{18}\text{O}$ values in the warmest environments could have been in the -5 to -8‰ range.

There are cogent arguments for¹⁰ and against¹¹ significant variations through time in seawater $\delta^{18}\text{O}$, but there is little consensus in that regard.

Interpretation of stable isotopic values for late Neoproterozoic carbonate rocks is certainly a challenge. But there are other plausible models to account for the extreme carbon and oxygen isotope values that are seen in some strata, and that seem to represent global patterns⁴. For example, one proposed explanation for extreme negative carbon-isotope perturbations in the Neoproterozoic, representing a significant decrease in the carbon-isotopic difference between carbonate carbon and organic carbon, is carbon transfer from a massive pool of dissolved organic carbon from anoxic deep waters to the dissolved inorganic carbon pool of the oceans¹². Another hypothesis to account for some of the same data is that enhanced oxidation of exposed organic-carbon-rich sediments on land resulted from a rise in atmospheric oxygen, with this ^{13}C -depleted dissolved inorganic carbon being incorporated into diagenetic carbonate cements in shallow-water limestones¹³.

Knauth and Kennedy's work¹ will prompt much discussion, and it will be some time before it becomes evident how valid their ideas are. Meanwhile, there is a message for researchers studying carbonate rocks from the Proterozoic: they may do well to view the diagenetic history of such rocks in light of the principles applied to carbonate rocks from the Phanerozoic.

Michael A. Arthur is in the Department of Geosciences and the Penn State Astrobiology Research Center, Pennsylvania State University, University Park, Pennsylvania 16802, USA.

e-mail: arthur@geosc.psu.edu

- Knauth, L. P. & Kennedy, M. J. *Nature* **460**, 728–732 (2009).
- Kennedy, M., Droser, M., Mayer, L. M., Pevear, D. & Mrofka, D. *Science* **311**, 1446–1449 (2006).
- Canfield, D. *Annu. Rev. Earth Planet. Sci.* **33**, 1–36 (2005).
- Hoffman, P. F. & Schrag, D. P. *Terra Nova* **14**, 129–155 (2002).
- Allan, J. R. & Matthews, R. K. *Sedimentology* **29**, 797–817 (1982).
- Land, L. S. *US Geol. Surv. Bull.* **1578**, 129–137 (1986).
- Lohmann, K. C. in *Paleokarst* (eds James, N. P. & Choquette, P. W.) 58–80 (Springer, 1988).
- Brand, U. & Veizer, J. *J. Sedim. Petrol.* **51**, 987–997 (1981).
- Jacobsen, S. B. & Kaufman, A. J. *Chem. Geol.* **161**, 37–57 (1999).
- Veizer, J. *et al. Chem. Geol.* **161**, 59–88 (1999).
- Muehlenbachs, K. *Chem. Geol.* **145**, 263–273 (1998).
- Rothman, D. H., Hayes, J. M. & Summons, R. E. *Proc. Natl Acad. Sci. USA* **100**, 8124–8129 (2003).
- Kaufman, A. J., Corsetti, F. A. & Varni, M. A. *Chem. Geol.* **237**, 47–63 (2007).

LETTERS

The late Precambrian greening of the Earth

L. Paul Knauth¹ & Martin J. Kennedy²

Many aspects of the carbon cycle can be assessed from temporal changes in the $^{13}\text{C}/^{12}\text{C}$ ratio of oceanic bicarbonate. $^{13}\text{C}/^{12}\text{C}$ can temporarily rise when large amounts of ^{13}C -depleted photosynthetic organic matter are buried at enhanced rates¹, and can decrease if phytomass is rapidly oxidized² or if low ^{13}C is rapidly released from methane clathrates³. Assuming that variations of the marine $^{13}\text{C}/^{12}\text{C}$ ratio are directly recorded in carbonate rocks, thousands of carbon isotope analyses of late Precambrian examples have been published to correlate these otherwise undatable strata and to document perturbations to the carbon cycle just before the great expansion of metazoan life. Low $^{13}\text{C}/^{12}\text{C}$ in some Neoproterozoic carbonates is considered evidence of carbon cycle perturbations unique to the Precambrian. These include complete oxidation of all organic matter in the ocean² and complete productivity collapse such that low- $^{13}\text{C}/^{12}\text{C}$ hydrothermal CO_2 becomes the main input of carbon⁴. Here we compile all published oxygen and carbon isotope data for Neoproterozoic marine carbonates, and consider them in terms of processes known to alter the isotopic composition during transformation of the initial precipitate into limestone/dolostone. We show that the combined oxygen and carbon isotope systematics are identical to those of well-understood Phanerozoic examples that lithified in coastal pore fluids, receiving a large groundwater influx of photosynthetic carbon from terrestrial phytomass. Rather than being perturbations to the carbon cycle, widely reported decreases in $^{13}\text{C}/^{12}\text{C}$ in Neoproterozoic carbonates are more easily interpreted in the same way as is done for Phanerozoic examples. This influx of terrestrial carbon is not apparent in carbonates older than ~ 850 Myr, so we infer an explosion of photosynthesizing communities on late Precambrian land surfaces. As a result, biotically enhanced weathering generated carbon-bearing soils on a large scale and their detrital sedimentation sequestered carbon⁵. This facilitated a rise in O_2 necessary for the expansion of multicellular life.

Carbonate is initially precipitated in the ocean as metastable calcite and/or aragonite, and is subsequently transformed into stable interlocking crystals of low-Mg calcite and/or dolomite. In this 'lithification' process, the originally precipitated phases undergo dissolution, reprecipitation, and isotopic re-equilibration with ambient pore fluids⁶. With the exception of rare, relatively well-preserved Phanerozoic shells, this happens to all carbonates. Precambrian carbonates are limestone or dolostone rocks; there are no preserved initial Precambrian marine precipitates.

On the basis of studies of Cenozoic deposits, lithification is most rapid in sediments in coastal areas where meteoric ground waters mix with marine pore fluids⁶. The process yields a roughly co-variant relationship between $\delta^{13}\text{C}$ and $\delta^{18}\text{O}$ in which $\delta^{13}\text{C}$ decreases as $\delta^{18}\text{O}$ decreases⁷⁻⁹ (Fig. 1a). The trend documents phases that formed in mixed meteoric/marine pore fluids. Meteoric waters are depleted in ^{18}O relative to ocean water, so $\delta^{18}\text{O}$ decreases with increasing proportions of meteoric water. Photosynthesizing communities living in coastal recharge areas preferentially fix ^{12}C , such that the biomass is

typically over 20‰ depleted in ^{13}C relative to the marine inorganic C reservoir. This ^{13}C -depleted C is incorporated into the meteoric water

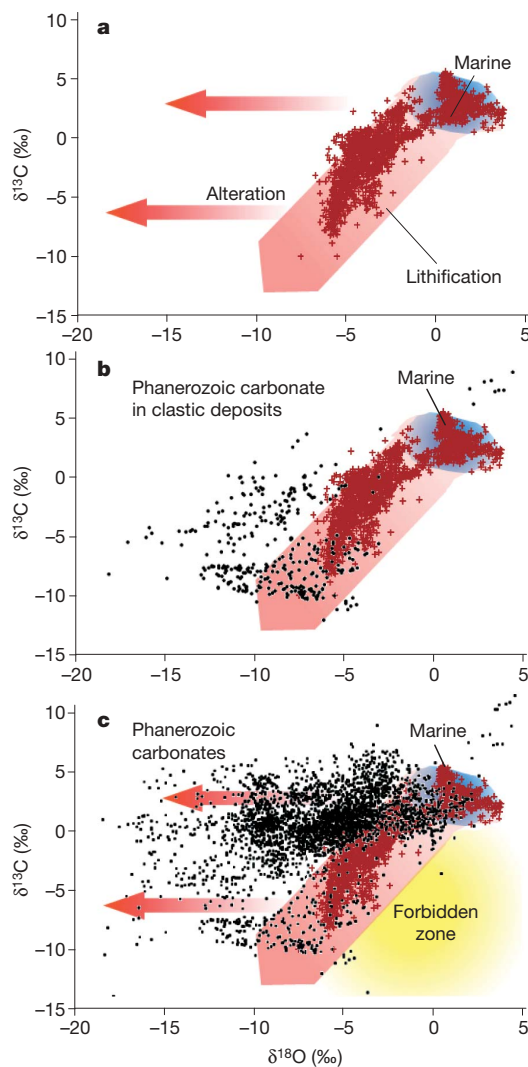


Figure 1 | Stable isotopes in Phanerozoic carbonates. **a**, Cenozoic limestones/dolostones form by way of solution/reprecipitation of primary marine precipitates. Blue area is dominantly marine pore fluids, red area contains significant meteoric water component. Both areas define the 'lithification' zone. Later deep burial and/or metamorphic alteration yield data to the left of the lithification domain, as shown by the arrows. **b**, Carbonate cements, lenses and beds in dominantly clastic successions. The lithification domain from **a** is shown in this and all subsequent figure panels for reference. **c**, Phanerozoic carbonates plot in or to the left of the lithification zone and avoid the forbidden zone. Data for this and all other figures are available in Supplementary Information.

¹School of Earth and Space Exploration, Arizona State University, Tempe, Arizona 85287-1404, USA. ²Department of Earth Science, University of California, Riverside, Riverside, California 92557, USA.

pore fluids through decomposition of the constantly renewing biomass and becomes incorporated into limestone/dolostone during lithification. A co-variation between $\delta^{18}\text{O}$ and $\delta^{13}\text{C}$ arises because low $\delta^{18}\text{O}$ signifies more meteoric water and thus a greater introduction of photosynthetically depleted ^{13}C from the subaerial recharge area. Pervasive intrusion of meteoric waters during sea-level fall is common on carbonate platforms. Pleistocene examples yield negative $\delta^{13}\text{C}$ and $\delta^{18}\text{O}$ over stratigraphic thicknesses $>100\text{ m}$ (ref. 7). $\delta^{13}\text{C}$ systematically decreases upward in the stratigraphic succession, like patterns widely reported for Neoproterozoic strata. The stratigraphic trend develops during lithification and is unrelated to any change in the global oceanic $\delta^{13}\text{C}$.

Carbonate rocks are susceptible to later recrystallization during deep burial, and can isotopically re-equilibrate with higher-temperature fluids depending upon the water/rock (W/R) ratios and the isotopic composition of the fluids. The W/R ratio of metamorphic fluids is typically high with respect to O and low with respect to C, so carbonate $\delta^{18}\text{O}$ is driven to lower values through higher-temperature equilibration while $\delta^{13}\text{C}$ undergoes little change¹⁰ (Fig. 1a). Ancient carbonates that form in coastal pore fluids and undergo later alteration

therefore display values that plot in, or to the left of, the lithification domain (Fig. 1a). Whereas $\delta^{13}\text{C}$ values as low as -10‰ can occur, most are greater than -5‰ . Low $\delta^{18}\text{O}$ of an ancient rock may have been set during the initial lithification event or during a much later metamorphic event. For example, a rock sample in the lithification domain (Fig. 1a) with $\delta^{18}\text{O} = -4\text{‰}$, $\delta^{13}\text{C} = -3\text{‰}$ does not represent the value of the initially precipitated marine sediment but does represent the initial, 'unaltered' value of the limestone or dolostone that formed during lithification. In Cenozoic rocks, its position in the crossplot would indicate that meteoric waters rich in coastal photosynthetic C were a component of the pore fluids during lithification. Neoproterozoic carbonate rocks should first be evaluated in this manner, which is well understood for Cenozoic limestone/dolostone formation.

Many published Neoproterozoic C isotope data are for dominantly clastic sections with relatively thin carbonate beds, cements and accumulations. Phanerozoic examples of carbonate in dominantly clastic sequences also display wide variations in $\delta^{18}\text{O}$ and $\delta^{13}\text{C}$ (Fig. 1b). In some successions, the isotopic signal is set during lithification in isotopically evolving pore fluids, as discussed above.

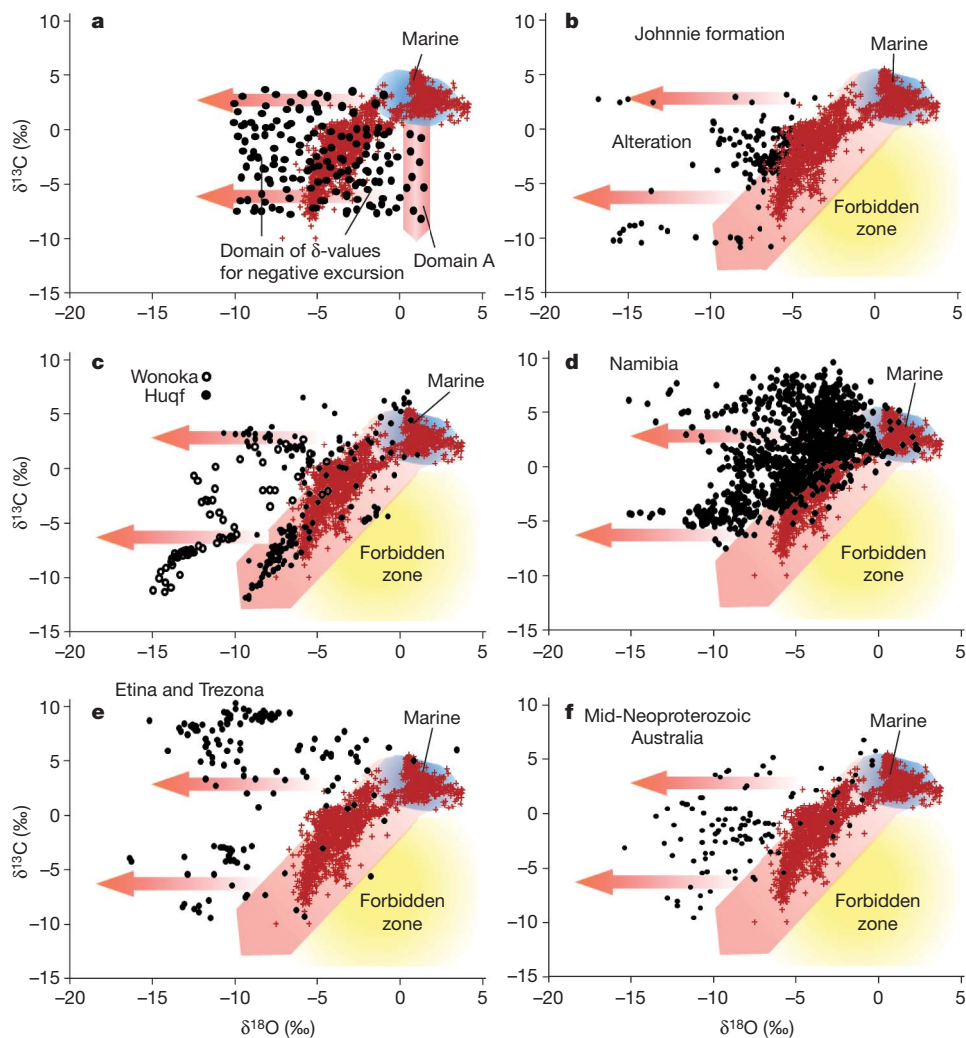


Figure 2 | Neoproterozoic carbonates. **a**, Data pattern expected for marine carbonates during a negative excursion of the global marine inorganic C reservoir. $\delta^{18}\text{O}$ of sea water is unaffected, so initial precipitates have marine $\delta^{18}\text{O}$ and progressively lower $\delta^{13}\text{C}$ depending upon the magnitude of the negative excursion (domain A). Subsequent alteration shifts the values to

lower $\delta^{18}\text{O}$. No forbidden zone occurs. **b–f**, Data for claimed negative C excursions all plot in or to the left of the forbidden zone. **b**, Johnnie Formation, USA; **c**, Wonoka Formation (Australia) and Huqf Group (Oman); **d**, Namibia (Africa); **e**, Etina and Trezona Formations (Australia); and **f**, Mid-Neoproterozoic (Australia).

For example, low $\delta^{18}\text{O}$ in carbonate-cemented shelf sands and silts results from meteoric waters in phreatic lenses, and low $\delta^{13}\text{C}$ is contributed from the terrestrial phytomass¹¹. More commonly, circulating deep basinal fluids produce late carbonate cements and lenses during burial. These have low $\delta^{18}\text{O}$ from equilibration with pore fluids at elevated temperatures, and $\delta^{13}\text{C}$ typically less than -5% from thermal decarboxylation of buried organic matter encountered along the fluid flow path^{12,13}. In all cases, the data plot near or to the left of the lithification reference domain (Fig. 1b).

In clastic-dominated sequences, the pore fluid W/R ratio for C is much larger than in limestone/dolostone sections. Any initial carbonate precipitates are therefore more susceptible to alteration of the C isotope ratio. Modern phreatic lenses over 100 m thick occur today in clastic sequences out to 100 km offshore¹⁴. Submarine groundwater flux rates through these lenses even exceed river runoff¹⁵. Such lenses migrate as a band across the shelf that tracks sea-level variation and exposes the vast majority of clastic shelf sediment to meteoric waters at some point during burial^{11,16}. Shelf sediments dominate past successions preserved in the stratigraphic record, so thick clastic sequences with low- $\delta^{18}\text{O}$, low- $\delta^{13}\text{C}$ carbonate are expected.

The pattern of lithification followed by possible later metamorphism results in a forbidden zone, which contains little data, located to the right of the lithification zone on the isotopic crossplot. Thousands of published analyses of Phanerozoic carbonates clearly avoid the forbidden zone (Fig. 1c). The majority of these data are for carbonate-dominated systems and thus have $\delta^{13}\text{C} > -5\%$.

Thousands of $\delta^{13}\text{C}$ analyses have now been published for Neoproterozoic carbonates to possibly correlate strata and explore for perturbations to the global C cycle. As observed in the Pleistocene⁷, thick intervals of negative $\delta^{13}\text{C}$ values occur in the Neoproterozoic but are considered to record profound perturbations to the global marine carbon cycle unique to the Neoproterozoic rather than being considered in terms of normal mixed meteoric/marine lithification or decarboxylation. In some cases, stratigraphic relations require these excursions to be sustained for millions of years at values even below the mantle average of -5% , the minimum value for a steady state C isotope mass balance in the Phanerozoic ocean¹⁷.

The relationship between $\delta^{13}\text{C}$ and $\delta^{18}\text{O}$ provides a useful means of distinguishing meteoric and burial lithification from marine excursions. Putative changes in the $\delta^{13}\text{C}$ of the ocean relate only to the well-mixed dissolved inorganic C reservoir, and show no relationship to $\delta^{18}\text{O}$ because the $\delta^{18}\text{O}$ of sea water is affected by totally different processes. A perturbation to the global C cycle that lowers the $\delta^{13}\text{C}$ of the surface ocean's dissolved inorganic C reservoir by claimed values of 5–12‰ (for example, ref. 2) therefore yields a negative excursion with values that would plot in the forbidden zone. Indeed, such excursions would define a vertical band for the precipitated carbonate as the excursion progressed down from the normal marine carbonate values (Fig. 2a). If the $\delta^{13}\text{C}$ of the precipitate is inviolate as currently assumed, later alteration drives $\delta^{18}\text{O}$ to lower values and a 'box-like' data array results, bounded to the right by the vertical excursion trajectory (Fig. 2a, domain A). This array is therefore expected, in contrast with that observed for the Phanerozoic.

Five classic examples of successions claiming to represent marine negative C isotope excursions do not show the expected crossplot for such excursions (Fig. 2b–f). Instead, they are bounded by the Cenozoic lithification domain to the right, and stream off to lower $\delta^{18}\text{O}$ values that are readily attributable to later metamorphic alteration. In all cases, the lower $\delta^{13}\text{C}$ values are associated with lower $\delta^{18}\text{O}$ values.

These data are incompatible with the excursion scenario unless (1) carbonates deposited during a negative $\delta^{13}\text{C}$ excursion are more susceptible to later $\delta^{18}\text{O}$ metamorphic alteration in proportion to their negative $\delta^{13}\text{C}$ value, or (2) $\delta^{18}\text{O}$ of sea water decreases as $\delta^{13}\text{C}$ of sea water decreases to produce an array that fortuitously resembles the Cenozoic lithification domain (Fig. 1a). There is no known geological mechanism compatible with the first scenario, and the second

would require synchronous changes of $>8\%$ in the $\delta^{18}\text{O}$ of sea water during the time of the putative C isotope excursions. No mechanisms that synchronously change oceanic $\delta^{18}\text{O}$ are known or have been proposed. The alternative explanation—that the Neoproterozoic carbonates underwent the same processes of lithification and metamorphism observed in Phanerozoic carbonates—is a simpler explanation for these data, and does not require extraordinary and anomalous behaviour of the C cycle specific to the Neoproterozoic.

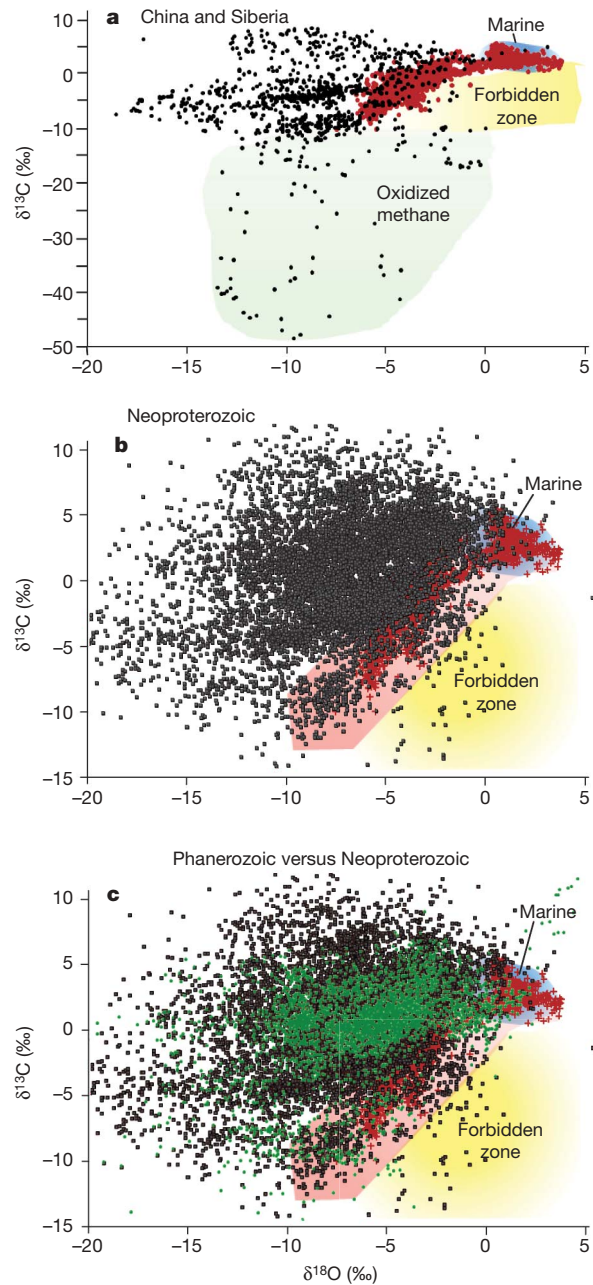


Figure 3 | All Neoproterozoic and Phanerozoic carbonates. **a**, Extreme ^{13}C depletions associated with oxidation of methane in samples from China and Siberia. Note expanded vertical scale. **b**, All published Neoproterozoic data. Nearly all plot in or to the left of the lithification reference domain. Most of the few values plotting in the forbidden zone probably represent unusual examples involving oxidation of methane, as documented for the China and Siberia forbidden zone samples. **c**, Comparison of Phanerozoic carbonates (green points) with Neoproterozoic carbonates. The data are isotopically indistinguishable.

Some Neoproterozoic carbonates with $\delta^{13}\text{C}$ as low as -40% do plot in the forbidden zone (Fig. 3a), but most of these have been attributed to local oxidation of methane^{3,18}. All unfiltered, published Neoproterozoic data (over 8,000 samples; references in Supplementary Information) yield very few samples in the forbidden zone (Fig. 3b). Several of those that do are thin horizons in otherwise low- ^{13}C intervals, and several are for claimed glaciomarine concretions¹⁹. The Neoproterozoic data are essentially indistinguishable from the Phanerozoic data (Fig. 3c). Similar to their Phanerozoic counterparts, carbonate sequences have $\delta^{13}\text{C} > -5\%$, whereas clastic sequences yield $\delta^{13}\text{C}$ as low as -10% . Rather than indicating C isotope excursions, the Neoproterozoic data seem to represent normal isotope variations that occur during lithification and metamorphism. Apparent correlations of low $\delta^{13}\text{C}$ between widely separated sections may relate simply to eustatic sea-level drops where phreatic lenses intrude simultaneously during lithification.

Consequences of this interpretation include: (1) $\delta^{18}\text{O}$ values of Neoproterozoic sea water were similar to that of the Cenozoic, consistent with the Muehlenbachs model²⁰; (2) a terrestrial phytomass existed that was large enough to inject enough photosynthetic C into coastal ground waters to produce identical C isotope depletions in marine carbonate to those observed in the Phanerozoic. The nature of the photosynthesizers is obscured by the absence of preserved terrestrial surfaces, although molecular and other evidence suggest the expansion of a primitive land biota starting at least by 1 Gyr ago^{5,21–23}. It was probably composed of protists, mosses, fungi and liverworts with evidence of lichen by 600 Myr ago^{5,24}. (3) Marine $\delta^{13}\text{C}$ may have varied in the Neoproterozoic, but this could only be deduced following careful consideration of large isotopic changes that occur during lithification and later alteration. The most positive $\delta^{13}\text{C}$ in a co-variant data array is the best minimum estimate of the marine $\delta^{13}\text{C}$ of the local marine depositional environment. This approach was used in one early study²⁵, and similar analysis is now warranted for all other Neoproterozoic sections.

If the first expansion of photosynthesizing communities on the land surface occurred in the Neoproterozoic, then carbonates deposited before 850 Myr ago should not show significant negative $\delta^{13}\text{C}$ values. Indeed, they cluster around $\delta^{13}\text{C} = 0 \pm 2\%$ (Fig. 4). Any earlier coastal phytomass was apparently not significant enough to produce strongly negative $\delta^{13}\text{C}$ in carbonates during the stabilization process.

The contrasting isotope data between 850 Myr ago and the Neoproterozoic suggest that the terrestrial expansion of photosynthesizing communities preceded the significant climate perturbations of

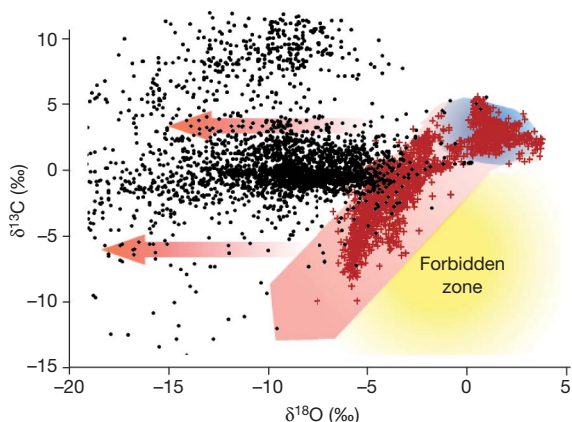


Figure 4 | Pre-850 Myr ago marine calcite and dolomite. These data do not display the ^{13}C depletions associated with lithification as observed for younger carbonates. Low ^{13}C was not being introduced during lithification, indicating minimal photosynthesizing communities on land in coastal areas. Being much older, these have undergone significantly more metamorphism to lower $\delta^{18}\text{O}$ values. Most of the very low $\delta^{13}\text{C}$ values are for vein-rich samples or high-grade metamorphic rocks.

the late Precambrian glaciations, and was followed by a rise of O_2 (ref. 26) and a secular change in terrestrial sediment composition⁵. The onset of significant biotically enhanced terrestrial weathering would have increased the flux of lithophile nutrient elements and clay minerals to continental margins. This would have increased production and burial preservation of organic C towards modern values^{5,27,28} and consequently facilitated the stepwise rise in atmospheric O_2 necessary to support multicellularity. The terrestrial expansion of an extensive, simple land biota indicated by the isotope data may thus have been a critical step in the transition from the Precambrian to the Phanerozoic world.

METHODS SUMMARY

All data plotted in the figures were extracted entirely from the published literature and online databases. All known Neoproterozoic data published as of 2008 were compiled without filtering or exclusion. The accompanying Excel file (Supplementary Information) lists all data and references for convenient reconstruction of the figures.

Received 20 June 2008; accepted 18 June 2009.

Published online 8 July 2009.

- Scholle, P. A. & Arthur, M. A. Carbon isotope fluctuations in Cretaceous pelagic limestones: potential stratigraphic and petroleum exploration tool. *Am. Assoc. Petrol. Geol. Bull.* **64**, 67–87 (1980).
- Fike, D. A., Grotzinger, J. P., Pratt, L. M. & Summons, R. E. Oxidation of the Ediacaran Ocean. *Nature* **444**, 744–747 (2006).
- Jiang, G. Q., Kennedy, M. J. & Christie-Blick, N. Stable isotopic evidence for methane seeps in Neoproterozoic postglacial cap carbonates. *Nature* **426**, 822–826 (2003).
- Hoffman, P. F., Kaufman, A. J., Halverson, G. P. & Schrag, D. P. A Neoproterozoic snowball earth. *Science* **281**, 1342–1346 (1998).
- Kennedy, M., Droser, M., Mayer, L. M., Pevear, D. & Mrofka, D. Late Precambrian oxygenation; inception of the clay mineral factory. *Science* **311**, 1446–1449 (2006).
- Land, L. S. Limestone diagenesis — some geochemical considerations. *US Geol. Surv. Bull.* **1578**, 129–137 (1986).
- Melim, L. A., Swart, P. K. & Maliva, R. G. in *Subsurface Geology of a Prograding Carbonate Platform Margin, Great Bahama Bank: Results of the Bahamas Drilling Project* Vol. 70 (ed. Ginsburg, R.N.) 137–161 (SEPM, 2001).
- Quinn, T. M. Meteoric diagenesis of Plio-Pleistocene limestones at Enewetak Atoll. *J. Sedim. Petrol.* **61**, 681–703 (1990).
- Gross, M. G. & Tracey, J. I. Oxygen and carbon isotopic composition of limestones and dolomites, Bikini and Eniwetok Atolls. *Science* **151**, 1082–1084 (1966).
- Banner, J. L. & Hanson, G. N. Calculation of simultaneous isotopic and trace-element variations during water-rock interaction with applications to carbonate diagenesis. *Geochim. Cosmochim. Acta* **54**, 3123–3137 (1990).
- Taylor, K. G., Gawthorpe, R. L., Curtis, C. D., Marshall, J. D. & Awwiller, D. N. Carbonate cementation in a sequence-stratigraphic framework: Upper Cretaceous sandstones, Book Cliffs, Utah–Colorado. *J. Sedim. Res.* **70**, 360–372 (2000).
- Hendry, J. P., Wilkinson, M., Fallick, A. E. & Haszeldine, R. S. Ankerite cementation in deeply buried Jurassic sandstone reservoirs of the central North Sea. *J. Sedim. Res.* **70**, 227–239 (2000).
- Fayek, M. *et al.* In situ stable isotopic evidence for protracted and complex carbonate cementation in a petroleum reservoir, North Coles Levee, San Joaquin Basin, California, USA. *J. Sedim. Res.* **71**, 444–458 (2001).
- Hathaway, J. C. *et al.* United States Geological Survey core drilling on the Atlantic Shelf. *Science* **206**, 515–527 (1979).
- Moore, W. S. S. a. r. m. i. e. n. t. o. J. L. & Key, R. M. Submarine groundwater discharge revealed by ^{228}Ra distribution in the upper Atlantic Ocean. *Nature Geosci.* **1**, 309–311 (2008).
- Brooks, S. M. & Whitaker, F. F. Geochemical and physical controls on vadose zone hydrology of Holocene carbonate sands, grand Bahama Island. *Earth Surf. Process. Landforms* **22**, 45–58 (1997).
- Bristow, T. F. & Kennedy, M. J. Carbon isotope excursions and the oxidant budget of the Ediacaran atmosphere and ocean. *Geology* **36**, 863–866 (2008).
- Pokrovskii, B. G., Melezhik, V. A. & Bujakaite, M. I. Carbon, oxygen, strontium, and sulfur isotopic compositions in late Precambrian rocks of the Patom Complex, central Siberia: Communication 2. Nature of carbonates with ultralow and ultrahigh $\delta^{13}\text{C}$ values. *Lithol. Miner. Res.* **41**, 576–587 (2006).
- Fairchild, I. J. & Spiro, B. Carbonate minerals in glacial sediments: geochemical clues to palaeoenvironment. *Geol. Soc. Lond. Spec. Publ.* **53**, 201–216 (1990).
- Muehlenbachs, K. The oxygen isotopic composition of the oceans, sediments and the seafloor. *Chem. Geol.* **145**, 263–273 (1998).
- Horodyski, R. J. & Knauth, L. P. Life on land in the Precambrian. *Science* **263**, 494–498 (1994).
- Heckman, D. S. *et al.* Molecular evidence for the early colonization of land by fungi and plants. *Science* **293**, 1129–1133 (2001).